Frequency-dependent shear viscosity, sound velocity, and sound attenuation near the critical point in liquids. III. The shear viscosity

G. Flossmann,[1] R. Folk,[1] and G. Moser[2]
[1]*Institute for Theoretical Physics, University of Linz, Linz, Austria*
[2]*Institute for Physics and Biophysics, University of Salzburg, Salzburg, Austria*
(Received 24 September 1998)

We compare theoretical results for the shear viscosity calculated in one-loop order within the field-theoretical method of the renormalization-group theory with experiments. Our expressions describe the nonasymptotic crossover in both temperature and density, and allow us to consider effects of finite gravitation and finite frequency at which the experiments are performed. In doing so we treat the critical exponent x_η of the shear viscosity as an independent parameter, keeping the one-loop value of the Kawasaki amplitude fixed. Within our model we also consider the temperature and density dependence of the thermal diffusion including gravitational effects. [S1063-651X(99)11907-X]

PACS number(s): 64.60.Ht, 05.70.Jk, 62.60.+v, 64.70.Fx

I. INTRODUCTION

This paper is the third part of an investigation of dynamical critical effects in pure fluids [1,2]. Its aim is to analyze and predict the singular behavior of transport coefficients induced by fluctuations near the gas-liquid critical point. The theoretical results cover the whole region where these effects are observed, and thus describe the crossover from the constant background values of the transport coefficients to the asymptotic power laws resulting from the renormalization-group (RG) invariance of the dynamical model at T_c. Much progress in this respect has also been made by other treatments of this topic, in particular by the mode coupling theory (for the latest and most complete state of this theory, see Ref. [3]) and the decoupled mode theory [4–6]. So far many aspects have been considered only within this theoretical formulation, e.g., the behavior away from the critical density. Here we extend the RG calculations to cover this region also, and show that close to the critical point the expressions calculated in RG theory lead to the same quality of agreement with experiments as the mode coupling results. This, however, is achieved, in our opinion, by much simpler expressions, namely, the one-loop dynamical amplitude functions calculated within the field theoretical method of the RG theory.

In order to describe dynamical crossover effects in pure fluids, two dynamical parameters, the background value of one dynamical quantity and the renormalized dynamical coupling, have to be taken from experiments. In fact only the last parameter is needed if the ratio of the transport coefficient to its nonsingular temperature and density-dependent background value is considered rather than the transport coefficient itself. We find a multiplicative enhancement not only for the shear viscosity where such a form has been derived within the mode coupling theory [7], but also for the thermal diffusivity. This is a consequence of using the nonasymptotic expression for the Kawasaki amplitude.

The deviation of the dynamical coupling from its fixed point value governs the nonasymptotic effects in the form that the dependence of the transport coefficients on the deviation from the critical point ($T=T_c$, $\rho=\rho_c$, $\omega=0$) is found from the flow equation of the dynamic coupling and the experimental static correlation length. This temperature- and density-dependent correlation length is the most important input in our theoretical expressions for the transport coefficients beside the dynamic constants.

In paper II we extracted the dynamical background parameters from the shear viscosity, using strictly the one-loop expressions, in particular for the dynamical critical exponent x_η. This was sufficient for predicting the temperature dependence of other transport coefficients, although we had to exclude the region very near T_c where gravitational effects mask the true asymptotic behavior. But even without this disturbance we would have expected deviations from the one-loop critical exponent. Several values have been calculated for the exponent x_η, namely, 0.054 [8,9], 0.051 [10], 0.053 [11], 0.065 [11], 0.063 [12], and 0.04 [13], and it was remarked earlier [14,15] that an exact experimental determination of the exponent turns out to be very difficult since the true asymptotic behavior is realized nowhere in the experimental region due to crossover and gravitational effects. Taking this situation into account, we treat the dynamical exponent x_η as an additional free parameter to be determined by the shear viscosity close to the critical point.

Another important effect results from the finite frequency at which measurements of the shear viscosity are performed. At finite frequency the shear viscosity remains finite at T_c, and it is of interest if and under which circumstances these frequency effects and gravitational effects can be discriminated. The frequency dependence [16,17] has already calculated earlier within the decoupled mode theory.

II. TRANSPORT COEFFICIENTS AT ZERO FREQUENCY AND CRITICAL DENSITY

In the preceding papers [1,2] we have derived theoretical expressions for the shear viscosity $\overline{\eta}$ [Eq. (I.6.6)] and the thermal diffusivity D_T [Eq. (I.6.5.)] in one-loop order,

$$\overline{\eta}(t)=\frac{k_B T}{4\pi}\,\frac{\xi(t)}{f_t^2(t)\Gamma(t)}\left(1-\frac{f_t^2(t)}{36}\right), \tag{2.1}$$

$$D_T(t)=\xi^{-2}(t)\Gamma(t)\left(1-\frac{f_t^2(t)}{16}\right), \tag{2.2}$$

where T is the temperature, k_B the Boltzmann constant, and Γ the Onsager coefficient corresponding to the heat mode. $t=(T-T_c)/T_c$ is the relative temperature distance, and f_t the mode coupling parameter between the order parameter fluctuations and the transverse momentum density given by Eq. (I.5.4). The temperature dependence of the mode coupling and the Onsager coefficient is found solving the corresponding one-loop order renormalization-group equations [see Eqs. (I.4.36) and (I.4.40)]. The flow parameter of the renormalization-group equations is related to the correlation length $\xi(t)$, so that the solutions may be written as

$$f_t^2(t)=\frac{24}{19}\left[1+\frac{\xi(t_0)}{\xi(t)}\left(\frac{24}{19f_0^2}-1\right)\right]^{-1}, \tag{2.3}$$

$$\Gamma(t)=\Gamma_0\left(\frac{f_0^2\xi(t)}{f_t^2(t)\xi(t_0)}\right)^{18/19}, \tag{2.4}$$

with the initial conditions $\Gamma(t_0)=\Gamma_0$ and $f_t(t_0)=f_0$ at an arbitrary temperature distance $t=t_0$. The exponent of $\Gamma(t)$ in Eq. (2.4) is the one-loop expression of $1-x_\eta$. Therefore, we may replace the one-loop value by the general exponent to obtain

$$\Gamma(t)=\Gamma_0\left(\frac{f_0^2\xi(t)}{f_t^2(t)\xi(t_0)}\right)^{1-x_\eta} \tag{2.5}$$

instead of Eq. (2.4), allowing the use of other than one loop values in our expressions or to treat x_η as an additional free parameter which may be found from the limiting value of $\overline{\eta}$ reached in earthbound experiments at T_c, if the background values are known with sufficient accuracy. Changing the exponent consistently in all transport coefficients (we neglect the static exponent η) changes neither the fixed point value of the mode coupling constant nor its temperature dependence. In this way the nonasymptotic Kawasaki amplitude ratio $R(t)$ remains unchanged, and reaches the fixed point value $R^*=1.056$ [18] at T_c, which is in agreement with experiments in ^{3}He [19,20]. This consistency of the Kawasaki amplitude ratio is important, since we are then able to keep the amplitude relation between the shear viscosity and the thermal diffusivity (or conductivity) fixed at its (reasonable) one-loop value.

We may further simplify the expressions for the shear viscosity and the thermal diffusivity by writing Eqs. (2.1) and (2.2) in a multiplicative form. Therefore, we introduce the background constants $\overline{\eta}_0$ and D_0 at the temperature distance t_0,

$$\overline{\eta}_0=\frac{k_BT}{4\pi}\frac{\xi(t_0)}{f_0^2\Gamma_0}\left(1-\frac{f_0^2}{36}\right), \tag{2.6}$$

$$D_0=\xi^{-2}(t_0)\Gamma_0\left(1-\frac{f_0^2}{16}\right), \tag{2.7}$$

so that the viscosity and the diffusivity read

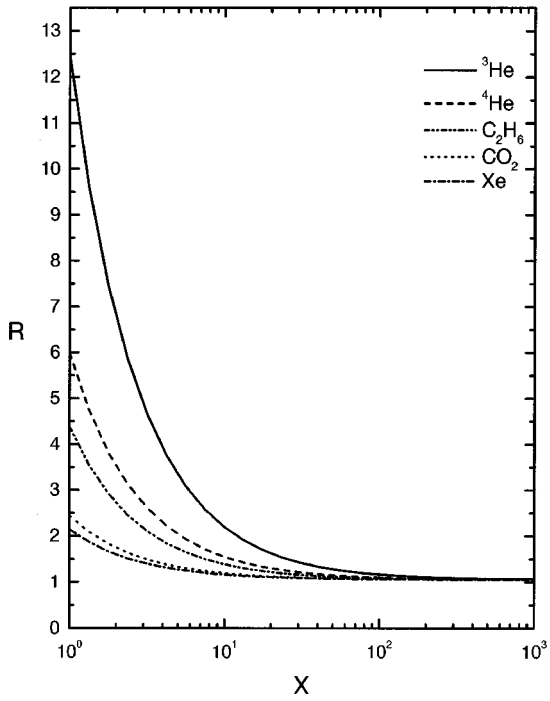

FIG. 1. Nonasymptotic Kawasaki amplitude as function of $X=\xi(t)/\xi(t_0)$ calculated from Eqs. (2.10) and (2.3) with the initial values taken from Table IV of Ref. [2]. Note that the critical point is approached if one goes to the right.

$$\overline{\eta}(t)=\overline{\eta}_0\frac{1-\frac{f_t^2(t)}{36}}{1-\frac{f_0^2}{36}}\left(\frac{f_0^2\xi(t)}{f_t^2(t)\xi(t_0)}\right)^{x_\eta}$$

$$\equiv\overline{\eta}_0\exp[x_\eta H(t)], \tag{2.8}$$

$$D_T(t)=D_0\frac{\xi^2(t_0)}{\xi^2(t)}\frac{\left(1-\frac{f_t^2(t)}{16}\right)}{\left(1-\frac{f_0^2}{16}\right)}\left(\frac{f_0^2\xi(t)}{f_t^2(t)\xi(t_0)}\right)^{x_\lambda}$$

$$\equiv D_0\exp[x_\lambda H_D(t)], \tag{2.9}$$

with $x_\lambda=1-x_\eta$. The reason why we can write the shear viscosity and thermal diffusivity in multiplicative forms is that we work from the beginning with the nonasymptotic Kawasaki amplitude given by

$$R_{\text{theor}}(t)=\frac{6\pi}{k_BT}D_T(t)\overline{\eta}(t)\xi(t)$$

$$=\frac{3}{2f_t^2(t)}\left(1-\frac{f_t^2(t)}{36}\right)\left(1-\frac{f_t^2(t)}{16}\right) \tag{2.10}$$

rather than with its asymptotic value R^*. In Fig. 1 we present the results of the nonasymptotic Kawasaki amplitude as a function of $\xi(t)/\xi(t_0)$ for various liquids. Equation (2.10) can easily be generalized [by replacing $\xi(t)$ by $\xi(t,\Delta\rho)$; see Sec. III] to noncritical values of the density so

that the curves shown in Fig. 1 are generally valid for zero frequency and zero gravity. We shall also note here that the background value D_0 is already fixed by the background value $\overline{\eta}_0$ of the shear viscosity,

$$D_0 = \overline{\eta}_0^{-1} \frac{k_B T}{4\pi} \frac{1}{f_0^2 \xi(t_0)} \left(1 - \frac{f_0^2}{16}\right)\left(1 - \frac{f_0^2}{36}\right). \quad (2.11)$$

A multiplicative form such as Eq. (2.8) was first calculated within mode coupling theory [7], and was improved later [3]. The crossover function H introduced in the mode coupling theory and now calculated by renormalization-group theory,

$$H(t) = \frac{1}{x_\eta} \ln\left(\frac{1 - \frac{f_t^2(t)}{36}}{1 - \frac{f_0^2}{36}}\right) + \ln\left(\frac{f_0^2 \xi(t)}{f_t^2(t)\xi(t_0)}\right), \quad (2.12)$$

has the proper limits $H=0$ at t_0 and $H \sim \nu \ln t$. The same limiting values are obtained for H_D given by

$$H_D(t) = \frac{1}{x_\lambda} \ln\left(\frac{1 - \frac{f_t^2(t)}{16}}{1 - \frac{f_0^2}{16}}\right) + \ln\left(\frac{f_0^2 \xi(t)}{f_t^2(t)\xi(t_0)}\right) + \frac{2}{x_\lambda} \ln\left(\frac{\xi(t_0)}{\xi(t)}\right). \quad (2.13)$$

H and H_D are not scaling functions, since they depend on the nonuniversal background parameter f_0. In Fig. 2 we compare our expression for H with the result of the mode coupling theory [3]. Therefore, we plot H as function of the dimensionless length $\xi(t)/\xi(t_0)$, where $\xi(t_0)$ is fixed so that the only free parameter is the initial value of the mode coupling f_0. In the mode coupling theory, however, H is a function of the dimensionless correlation length $q_D \xi(t)$ with one free fit parameter q_D. There is another important difference between the mode coupling theory and our result. In Eq. (2.8) we use the background constant $\overline{\eta}_0$, which is the value of the shear viscosity at t_0 once that the analytic background temperature dependence has been subtracted (see Sec. VI for details) whereas in the mode coupling theory the full regular background $\overline{\eta}^{reg}(T)$ is used instead of $\overline{\eta}_0$. So Eqs. (2.8) and (2.9) only describe the purely singular part of the transport coefficients without any contribution of the temperature-dependent background. We mention here that the theoretical expression for the thermal conductivity $\kappa_T = \rho C_P D_T$ is obtained from the diffusivity by multiplying with the density ρ and the specific heat at constant pressure C_P, as discussed in the preceding paper [2]. We do not take the theoretical expression for the specific heat but its experimental counterpart everywhere in our calculations.

In order to proceed with our calculation of the transport coefficients all we need at this stage is the two initial values Γ_0 and f_0, the initial temperature t_0 [21] and an explicit expression for the correlation length $\xi(t)$. The temperature dependence of the correlation length does not follow the asymptotic power law in general, but may include corrections to the leading terms in the crossover region. It would be worthwhile to measure the explicit crossover temperature dependence of $\xi(t)$ in order to perform the analysis in the background properly. However, lacking more detailed experimental information we will use the asymptotic expression

$$\xi(t) = \xi_0 t^{-\nu}, \quad (2.14)$$

which seems to be sufficient in the temperature region $t \leqslant 10^{-1}$ with respect to the uncertainties of other physical quantities entering the transport coefficients. The value of the universal critical exponent $\nu = 0.63$ [12] has been confirmed experimentally for several liquids [22]. For the calculation of the shear viscosity, we thus need a knowledge of three nonuniversal parameters ξ_0, Γ_0, and f_0. The amplitude of the correlation length ξ_0 has been determined experimentally for several fluids, and is listed together with the critical temperature T_c and the critical density ρ_c in Table I for the liquids considered in the following. For a comprehensive overview on experimental results in several other liquids, see Ref. [22] and the references therein.

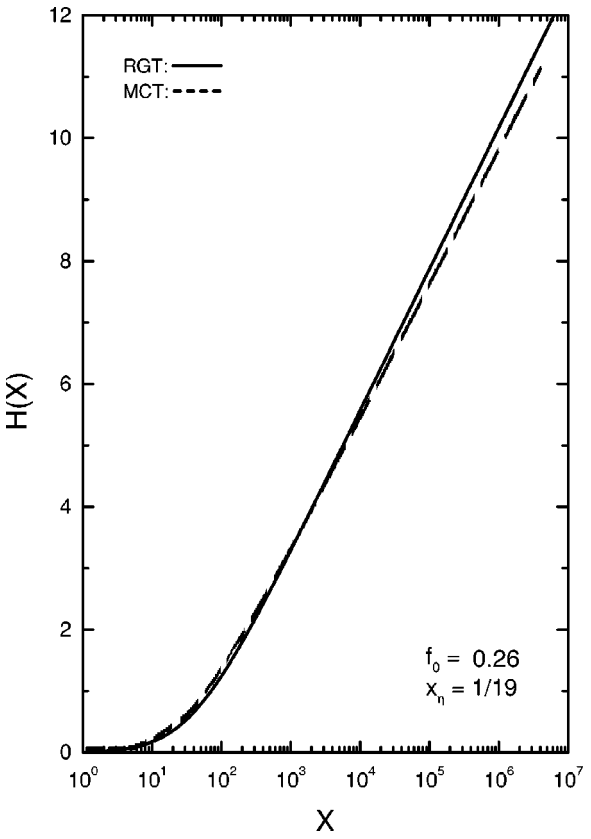

FIG. 2. Comparison of the renormalization-group result for the function H of Eq. (2.8) with the mode coupling result of Ref. [3] (see Fig. 3 there): X is $\xi(t)/\xi(t_0)$ in renormalization-group theory, and $q_D \xi(t)$ in mode coupling theory.

III. TRANSPORT COEFFICIENTS AT ZERO FREQUENCY AND NONCRITICAL DENSITY

In order to extend our model to noncritical values of the density, we need an equation of state close to the critical

TABLE I. Nonuniversal parameters of several fluids.

Liquid	ξ_0 (Å)	T_c (K)	ρ_c (g/cm^3)	P_c (10^{-6}g/cm s^2)	h_c (10^{-6} cm)	a	k
^{3}He	2.7	3.3086	0.0414	1.1678	0.116	4.05	0.818
^{4}He	2.0	5.1895	0.0696	2.2742	0.189	5.66	0.904
C_2H_6	1.9	305.33	0.2066	48.718	4.303	17.9	1.255
CO_2	1.6	304.119	0.4664	73.753	3.047	18.9	1.273

point to find the correlation length ξ as a function of the temperature and density. To do this we apply the cubic model discussed in the Appendix. The temperature- and density-dependent shear viscosity $\overline{\eta}(t,\Delta\rho)$ and thermal diffusivity $D_T(t,\Delta\rho)$ are then obtained inserting the full correlation length $\xi(t,\Delta\rho)$ given by Eq. (A4) into Eqs. (2.3), (2.8), and (2.9),

$$\overline{\eta}(t,\Delta\rho)=\overline{\eta}_0\frac{1-\dfrac{f_t^2(t,\Delta\rho)}{36}}{1-\dfrac{f_0^2}{36}}\left(\frac{f_0^2\xi(t,\Delta\rho)}{f_t^2(t,\Delta\rho)\xi(t_0)}\right)^{x_\eta}$$

$$\equiv\overline{\eta}_0 g_\eta(t,\Delta\rho), \tag{3.1}$$

$$D_T(t,\Delta\rho)=D_0\frac{\xi^2(t_0)}{\xi^2(t,\Delta\rho)}\times\frac{\left(1-\dfrac{f_t^2(t,\Delta\rho)}{16}\right)}{\left(1-\dfrac{f_0^2}{16}\right)}\left(\frac{f_0^2\xi(t,\Delta\rho)}{f_t^2(t,\Delta\rho)\xi(t_0)}\right)^{x_\lambda}$$

$$\equiv D_0 g_D(t,\Delta\rho), \tag{3.2}$$

where $\Delta\rho$ is the reduced density defined in Eq. (A2). Let us note here that, strictly speaking, the relations $\overline{\eta}_0=\overline{\eta}(t_0)$ and $D_0=D_T(t_0)$ are only correct along the critical isochore, but if t_0 is chosen far enough away from the critical point where we have $\xi(t_0,\Delta\rho)\simeq\xi(t_0)$, we find

$$\overline{\eta}(t_0,\Delta\rho)=\overline{\eta}_0\frac{1-\dfrac{f_t^2(t_0,\Delta\rho)}{36}}{1-\dfrac{f_0^2}{36}}\left(\frac{f_0^2\xi(t_0,\Delta\rho)}{f_t^2(t_0,\Delta\rho)\xi(t_0)}\right)^{x_\eta}\approx\overline{\eta}_0, \tag{3.3}$$

$$D_T(t_0,\Delta\rho)=D_0\frac{\xi^2(t_0)}{\xi^2(t_0,\Delta\rho)}\times\frac{\left(1-\dfrac{f_t^2(t_0,\Delta\rho)}{16}\right)}{\left(1-\dfrac{f_0^2}{16}\right)}\left(\frac{f_0^2\xi(t_0,\Delta\rho)}{f_t^2(t_0,\Delta\rho)\xi(t_0)}\right)^{x_\lambda}$$

$$\approx D_0, \tag{3.4}$$

with an error of the order of 1% in the region considered. So $\overline{\eta}_0$ and D_0 may still be considered as the values of the shear viscosity and the thermal diffusivity at $t=t_0$, neglecting the regular density and temperature dependence. Thus our expressions for the transport coefficients have to be identified with the experimental values after subtracting the regular temperature- and density-dependent parts, and adding the regular value at T_c and ρ_c (see Sec. VI).

As the cubic model expression for the correlation length (A4) is symmetric around the critical isochore, so are Eqs. (3.1) and (3.2), as they only describe the purely singular part of the transport coefficients. On the other hand, we may introduce density-dependent background values $\overline{\eta}_0(\Delta\rho)$ and $D_0(\Delta\rho)$ allowing a density dependence of the Onsager coefficient $\Gamma_0(\Delta\rho)$ instead of correcting the experimental data for their analytic density-dependent background. This dependence is then fixed by the constraint that the background value of the transport coefficient should coincide with the background value of the experimental transport coefficient at t_0,

$$\Gamma_0(\Delta\rho)\simeq\frac{k_BT}{4\pi}\frac{\xi(t_0)}{f_0^2\overline{\eta}^{\rm expt}(t_0,\Delta\rho)}\left(1-\frac{f_0^2}{36}\right). \tag{3.5}$$

A similar relation holds for the density-dependent background values of the transport coefficient. The theoretical expression for the normalized transport coefficient are then simply

$$\frac{\overline{\eta}(t,\Delta\rho)}{\overline{\eta}(t_0,\Delta\rho)}=g_\eta(t,\Delta\rho), \tag{3.6}$$

$$\frac{D_T(t,\Delta\rho)}{D_T(t_0,\Delta\rho)}=g_D(t,\Delta\rho). \tag{3.7}$$

IV. TRANSPORT COEFFICIENTS AT ZERO FREQUENCY AND NONZERO GRAVITY

Now we look at a liquid enclosed in a vessel of fixed height h. In nonzero gravity we find a density gradient in the liquid leading to a dependence of the correlation length, and thus of the shear viscosity and the thermal diffusivity on the vertical position in the vessel [20]. In experiments one usually measures the average shear viscosity or the average thermal diffusivity, but the way of averaging depends considerably on the experimental technique, as will be explained below.

The shear viscosity is usually measured in a vessel with two rotating discs at the bottom and top. Therefore, the average shear viscosity simply consists of the contributions of

the viscosity, or more precisely, the decrement $D \propto \sqrt{\eta\rho}$ at the bottom and the top. Adjusted to this experimental procedure, we define the average shear viscosity $\overline{\eta}_{\rm av}$ along the critical isochore as [20]

$$\overline{\eta}_{\rm av}(t) = \frac{(\sqrt{\overline{\eta}_b \rho_b} + \sqrt{\overline{\eta}_t \rho_t})^2}{4\rho_c}. \tag{4.1}$$

The above definition is only valid along the critical isochore and cannot be generalized to other isochores in a simple and straightforward way. The shear viscosity and the density at the bottom and at the top of the vessel at fixed temperature t simply read $\overline{\eta}_b = \overline{\eta}(\xi_b(t))$, $\overline{\eta}_t = \overline{\eta}(\xi_t(t))$, $\rho_b = \rho_c[1 + \Delta\rho_b(t)]$, and $\rho_t = \rho_c[1 + \Delta\rho_t(t)]$. The correlation lengths $\xi_{b,t}$ and the reduced densities $\rho_{b,t}$ at the bottom and top, which are both functions of the reduced temperature, can be evaluated in terms of the cubic model as explained in the Appendix. In experiments for the thermal diffusivity or the thermal conductivity, we usually average over the whole sample instead, so that the average thermal diffusivity $D_{T_{\rm av}}$ is found to be

$$D_{T_{\rm av}}(t, \overline{\Delta\rho}) = \int_{z_1}^{z_2} D_T[\xi(t, \Delta\rho(z))] dz, \tag{4.2}$$

with $\Delta\rho(z)$ the gravity-induced density profile, z the vertical coordinate introduced in the Appendix and z_1 and z_2, respectively, are the coordinates of the bottom and top of the vessel, now functions of the reduced temperature and the average reduced density. We shall note here that Eq. (4.2) is valid for <u>all</u> values of the average reduced density and not only for $\overline{\Delta\rho} = 0$ such as Eq. (4.1). In the Appendix we describe how to obtain the coordinates z_1 and z_2, and how to evaluate Eq. (4.2) numerically.

Exactly at the critical point we are able to evaluate Eq. (4.1) analytically using the cubic model expressions of the Appendix: Along the critical isotherm the parameters r and θ of the cubic model read

$$\theta = \mathrm{sgn}(z)\frac{1}{b} \quad \text{and} \quad r = \left[\frac{h|z|}{h_c(b^{-1} - b^{-3})}\right]^{1/\beta\delta}. \tag{4.3}$$

In addition, we know that along the critical isochore the vertical position of the bottom and the top of the vessel is always given by $z = \pm 1/2$, so that $\Delta\rho$ and ξ, given by Eqs. (A2) and (A4), respectively, take on the constant values

$$\Delta\rho_t = -\Delta\rho_b = k(b^{-1} + cb^{-3})\left[\frac{h/2}{h_c(b^{-1} - b^{-3})}\right]^{1/\delta} = 1.102\, k\left(\frac{h}{h_c}\right)^{1/\delta}, \tag{4.4}$$

$$\xi_t = \xi_b = \xi_0(1 + 0.16b^{-2})\left[\frac{h/2}{h_c(b^{-1} - b^{-3})}\right]^{-\nu/\beta\delta} = 0.783\,\xi_0\left(\frac{h}{h_c}\right)^{-\nu/\beta\delta}, \tag{4.5}$$

TABLE II. Universal parameters from [24].

α	β	γ	δ	ν	η	b	c
0.100	0.355	1.190	4.352	0.633	0.121	1.1446	0.0393

where we have applied the universal exponents and cubic model constants of Table II. The critical height h_c defined in the Appendix is listed in Table I for several liquids. Now we can insert Eq. (4.5) into Eq. (3.1) obtain the values of the shear viscosity at the top and bottom which we finally insert into Eq. (4.1) together with the expression for the reduced density [Eq. (4.4)] to end up with the average shear viscosity $\overline{\eta}_{\rm av}$, which takes on a constant value. Once f_0 is known from a fit of the nonasymptotic shear viscosity, or even better from a fit of the thermal diffusivity, this constant value allows the determination of the exponent x_η much more precisely than any fit in the asymptotic region. Unfortunately such experimental data are not available at the moment, but we have nevertheless plotted $\overline{\eta}_{\rm av}/\overline{\eta}_0$ exactly at the critical point in ^{3}He as a function of x_η for three different values of f_0 in Fig. 3 to give the reader an impression of the functional dependence. The sensitivity of the value of the shear viscosity T_c on the gravitation is also observed in the mode coupling theoretical analysis in Ref. [20]. Since the shear viscosity is already divided by its background value, no static quantities other than the correlation length enter into the comparison.

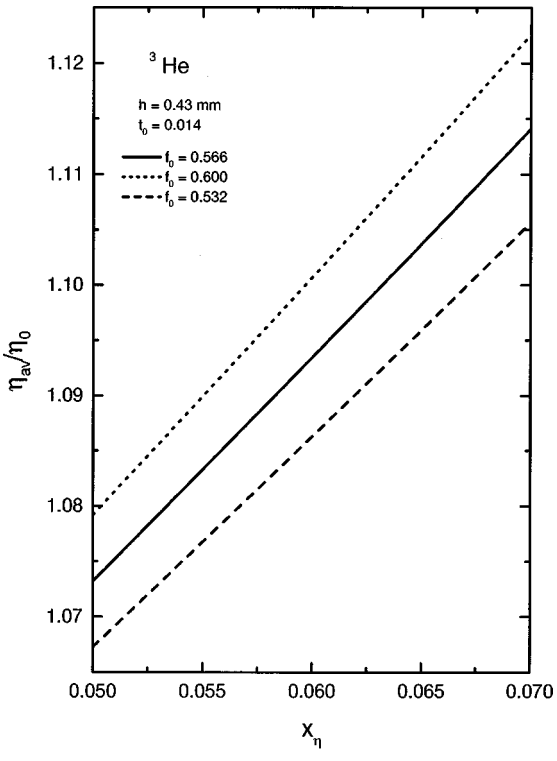

FIG. 3. Saturation value of the normalized shear viscosity $\overline{\eta}_{av}/\overline{\eta}_0$ of ^{3}He at the critical point under the influence of gravitation as a function of the the dynamical exponent x_η for various initial values f_0 of the dynamic coupling (the height of the vessel is $h = 0.43$ mm, and $t_0 = 0.014$). This shows that in an earthbound experiment the accuracy of the background values limits the accuracy of x_η.

V. FREQUENCY-DEPENDENT SHEAR VISCOSITY

In paper I of this series [1] we also derived the theoretical expressions for the frequency-dependent shear viscosity $\overline{\eta}$ [Eq. (I.5.7.)] and the frequency-dependent frictional coefficient β [Eq. (I.5.8.)]. Inserting the solution of the flow equation for the mode coupling g [Eq. (II.2.7) in [2]] with $\kappa = \xi_0^{-1}$ these expressions read

$$\overline{\eta}(t,\Delta\rho,\omega) = \frac{k_B T}{4\pi}\frac{\xi_0}{l f_t^2(l)\Gamma(l)}[1+E_t(f_t(l),v(l),w(l))], \tag{5.1}$$

$$\beta(t,\Delta\rho,\omega) \approx \frac{1}{4\pi N_A}\frac{\xi_0}{l f_t^2(l)\Gamma(l)}\{1+(\mathrm{Re}+\mathrm{Im}) \times[E_t(f_t(l),v(l),w(l))]\}, \tag{5.2}$$

As pointed out by Bhattacharjee and Ferrell [16] the quantity measured in experiments is not the complex shear viscosity but related to the frictional coefficient so that one has to take the sum of the real and the imaginary part of Eq. (5.1) in order to compare our results with experiments. The one-loop perturbational contribution is

$$\begin{aligned} E_t(f_t(l),v(l),w(l)) = &-\frac{f_t^2}{96}\Bigg\{1+6\Bigg[i\frac{v^2}{w}\ln v+\frac{1}{v_+-v_-}\left(\frac{v_-^2}{v_+}\ln v_- - \frac{v_+^2}{v_-}\ln v_+\right)\Bigg] \\ &-\frac{4}{(v_+-v_-)^3}\left[\frac{v_+^3-v_-^3}{3}+\frac{3}{2}(v_+-v_-)(v_+^2\ln v_+ + v_-^2\ln v_-)-(v_+^3\ln v_+ - v_-^3\ln v_-)\right] \\ &+\frac{2}{(v_+-v_-)^2}\Bigg[\frac{v_+^3}{v_-}(1+4\ln v_+)+\frac{v_-^3}{v_+}(1+4\ln v_-)+\left(\frac{1}{v_-}-\frac{2}{v_+-v_-}\right)\frac{v_+^4\ln v_+ - v^4\ln v}{v_-} \\ &+\left(\frac{1}{v_+}+\frac{2}{v_+-v_-}\right)\frac{v_-^4\ln v_- - v^4\ln v}{v_+}\Bigg]\Bigg\}, \end{aligned} \tag{5.3}$$

where we have dropped the argument l in the parameters on the right hand side of the equation. The parameters introduced in Eq. (5.3) are defined as

$$v(l) = \frac{\xi^{-2}(t)}{(\xi_0^{-1}l)^2}, \quad w(l,\omega) = \frac{\omega}{2\Gamma(l)(\xi_0^{-1}l)^4},$$

$$v_\pm(l,\omega) = \frac{v}{2} \pm \sqrt{\left(\frac{v}{2}\right)^2 + iw}. \tag{5.4}$$

The Onsager coefficient $\Gamma(l)$ and the mode coupling $f_t(l)$ now read

$$\Gamma(l) = \Gamma_0\left(\frac{19f_0^2}{24}\frac{l_0}{l}\left[1+\frac{l}{l_0}\left(\frac{24}{19f_0^2}-1\right)\right]\right)^{1-x_\eta}, \tag{5.5}$$

$$f_t(l) = \frac{24}{19}\left[1+\frac{l}{l_0}\left(\frac{24}{19f_0^2}-1\right)\right]^{-1}, \tag{5.6}$$

where Γ_0, f_0, and l_0 are the initial values of the Onsager coefficient Γ, the mode coupling f_t, and the flow parameter l, all determined at $t=t_0$ and $\Delta\rho=0$.

The mode coupling parameter l is a function of the temperature t, the density $\Delta\rho$ and the frequency ω and results from the solution of the matching condition [Eq. (I.5.28)],

$$\left(\frac{\xi_0}{\xi(t,\Delta\rho)}\right)^8 + \left(\frac{2\omega\xi_0^4}{\Gamma(l)}\right)^2 = l^8, \tag{5.7}$$

which can be solved numerically as the correlation length $\xi(t,\Delta\rho)$ and the Onsager coefficient $\Gamma(l)$ are given by Eqs. (A4) and Eq. (5.5), respectively. The initial value l_0 is found from Eq. (5.7) inserting $\xi(t_0)$ instead of $\xi(t,\Delta\rho)$.

Before we come to gravitational effects let us introduce an effective temperature distance $\overline{t}$, which is a function of the temperature distance t, the reduced density $\Delta\rho$, and the frequency ω, and is determined by the matching condition via an effective correlation length $\xi_{\mathrm{as}}(\overline{t}) = \xi_0 t^{-\nu}$:

$$\xi^{-8}(t,\Delta\rho) + \left(\frac{2\omega\xi_0^4}{\Gamma(\overline{t})}\right)^2 = \xi_{\mathrm{as}}^{-8}(\overline{t}). \tag{5.8}$$

The above equation allows the calculation of the corresponding effective temperature distance $\overline{t}$ for each real temperature distance t at finite frequency and density at which the values of the model parameters have to be known. In Fig. 4 the function $\overline{t}(t)$, calculated by inversion of Eq. (5.8) at fixed ω, is shown for several frequencies along the critical isochore. Approaching the critical temperature at finite frequencies, the effective temperature distance $\overline{t}$ becomes constant. Thus all static and dynamic parameters that are functions of the flow parameter also turn into constant values at T_c. A similar behavior of $\overline{t}$ is found at zero frequency when the density differs from its critical value. With the solution $\overline{t}(t,\Delta\rho,\omega)$ of Eq. (5.8) the temperature and frequency parameters in Eq. (5.4) can be rewritten as

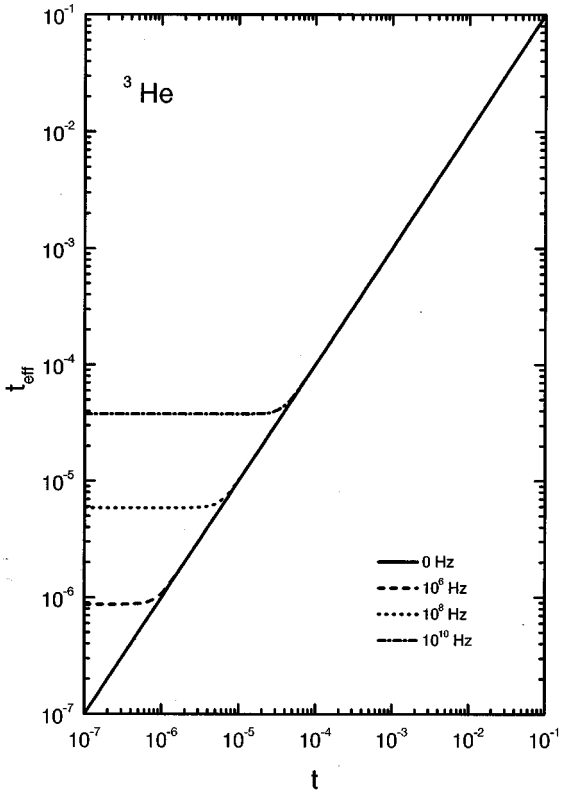

FIG. 4. Effective temperature distance t_{eff} vs real temperature difference t for ^{3}He for various frequencies at zero gravity along the critical isochore.

$$v(t,\bar{t})=\frac{\xi^{-2}(t)}{\xi^{-2}[\bar{t}]},\quad w(\bar{t})=\frac{\omega}{2\Gamma[\bar{t}]\xi^{-4}[\bar{t}]}. \tag{5.9}$$

The situation is a bit more complicated when gravitational effects are no longer neglected: Like before in the limit of vanishing frequency and on the critical isochore, we find the average shear viscosity $\bar{\eta}_{\mathrm{av}}(t,\omega)$ inserting the local values of the frequency-dependent shear viscosity (5.1) at the bottom and top into Eq. (4.1). But now this means that we need the flow parameter l not only as a function of the temperature, the density, and the frequency, but also of the vertical position z (e.g., the bottom and top) in the vessel. So in order to evaluate the frequency dependence at nonzero gravity we insert the correlation length $\xi(t,\Delta\rho(z))$ from the Appendix, and the Onsager coefficient $\Gamma(l)$, into the matching condition (5.8), which now reads

$$\left(\frac{\xi_0}{\xi(t,\Delta\rho(z))}\right)^8+\left(\frac{2\omega\xi_0^4}{\Gamma(l)}\right)^2=l, \tag{5.10}$$

with the solution $l(t,\Delta\rho(z),\omega)$ which we insert into Eq. (5.1) to find the shear viscosity $\bar{\eta}_{b,t}$ at the bottom and top, respectively. With gravitation we may define an effective temperature distance $\bar{t}(t,\Delta\rho(z),\omega)$ analogously to Eq. (5.8) at any position z in the vessel.

In Fig. 5 and 6 we plot the sum of the real and imaginary parts of the shear viscosity at various frequencies with and without gravitation in ^{3}He. There we see that even in a very small vessel of 0.1 mm, gravity effects cover up all frequency effects with $\omega<1$ kHz so that we can conclude that in earthbound experiments frequency effects will hardly be visible close to the critical point. Similar results for the frequency-dependent shear viscosity in zero gravity were already obtained within the mode coupling theory [17]. Our results for zero gravity but finite frequency agree with the curves shown in Fig. 9 of Ref. [20] which were calculated with the expressions derived in Ref. [17]. Unfortunately, experimental data are not available in a large enough frequency interval to compare them with our theoretical results, so that we have to stick to the zero frequency case in Sec. VI.

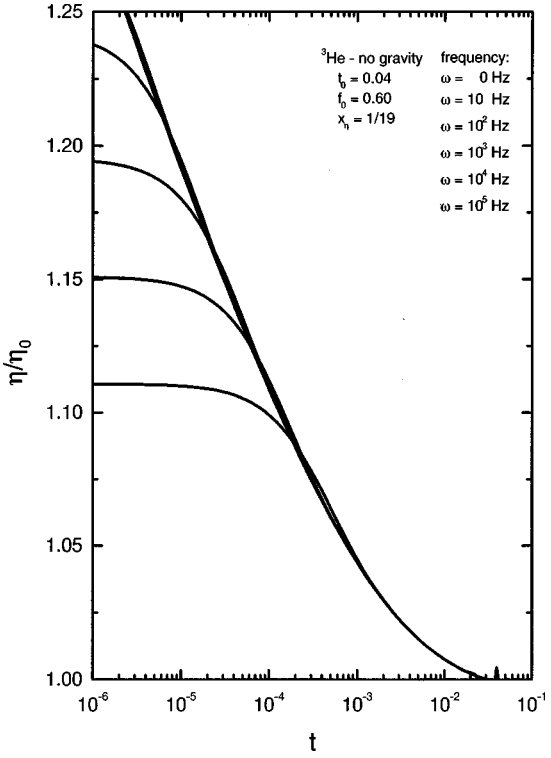

FIG. 5. Shear viscosity in ^{3}He along the critical isochore at various frequencies without gravitation.

VI. COMPARISON OF THE ZERO FREQUENCY TRANSPORT COEFFICIENTS WITH EXPERIMENTS

Before we discuss the results of the comparison of our theory with experiments, we shall describe how to fit the initial values of the Onsager coefficient Γ_0 and the mode coupling f_0 as well as the dynamic exponent x_η from experimental data for the shear viscosity and thermal diffusivity. Therefore, we have to discuss briefly the connection between our theoretical results and experimental data for these two quantities:

As discussed in Secs. II and III, the experimental transport coefficients consist of a singular part and a regular background part, both of them functions of the temperature and density. As the temperature and density dependence of the background part is not described within the RG theory, one has to correct the experimental data for this dependence in order to extend the region of fit into the region where the regular temperature and density dependence sets in. This can be done in the following way: From a fit of the shear viscosity outside the critical region, one determines the regular part

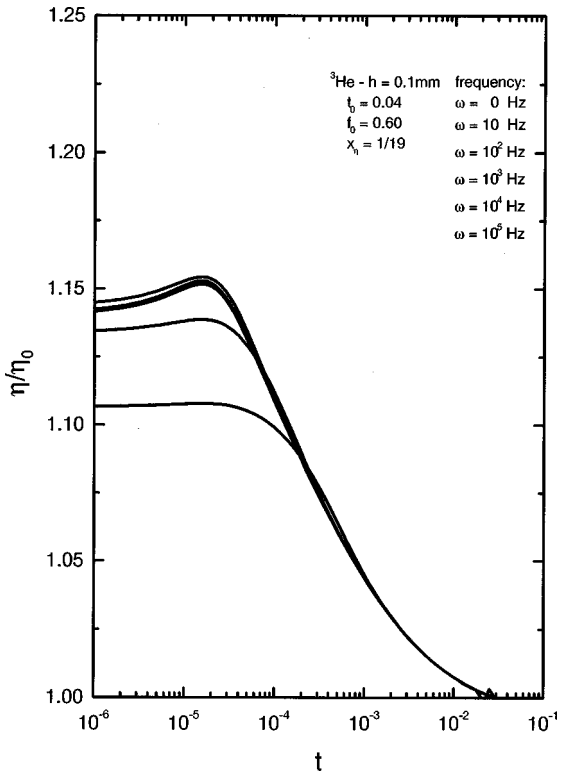

FIG. 6. Average shear viscosity in ^{3}He along the critical isochore at various frequencies with gravitation (the height of the cell is $h=0.1$ mm).

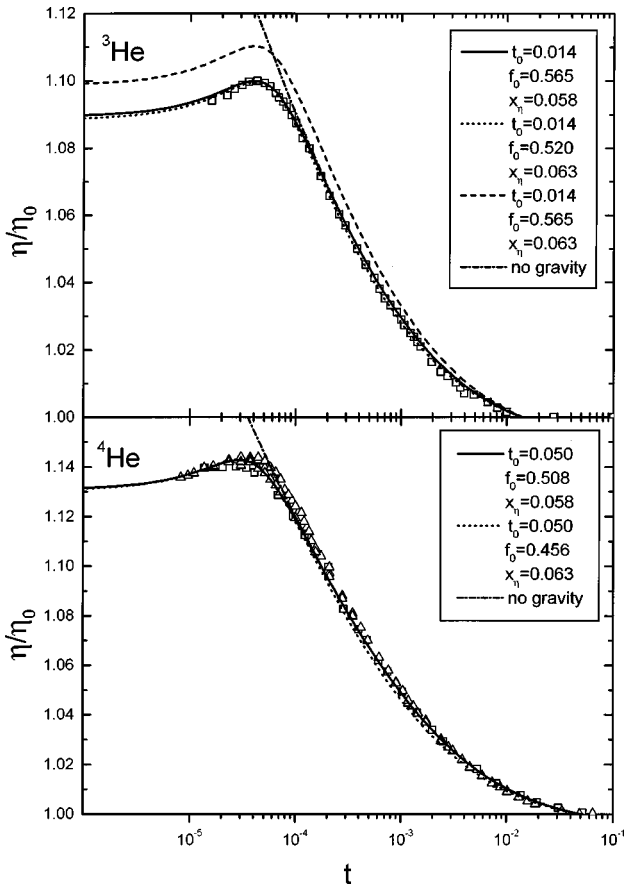

FIG. 7. Shear viscosity in ^{3}He (top) and ^{4}He (bottom) along the critical isochore with gravitation (full curve: $x_\eta=0.058$; dotted curve: $x_\eta=0.063$; dashed curve: $x_\eta=0.063$ and f_0 fitted from the thermal diffusivity) and without gravitation (dash-dotted curve). Experimental data are from Ref. [20].

$\overline{\eta}^{\rm reg}(t,\Delta\rho)$ of the shear viscosity and $D_T^{\rm reg}(t,\Delta\rho)$ of the thermal diffusivity. Then we subtract the regular part $\overline{\eta}^{\rm reg}(t,\Delta\rho)$ or $D_T^{\rm reg}(t,\Delta\rho)$, respectively, from the experimental data, and add the regular contribution $\overline{\eta}^{\rm reg}(0,0)$ or $D_T^{\rm reg}(0,0)$ exactly at the critical point;

$$\overline{\eta}^{\rm corr}(t,\Delta\rho)=\overline{\eta}^{\rm expt}(t,\Delta\rho)-\overline{\eta}^{\rm reg}(t,\Delta\rho)+\overline{\eta}^{\rm reg}(0,0), \tag{6.1}$$

$$D_T^{\rm corr}(t,\Delta\rho)=D_T^{\rm expt}(t,\Delta\rho)-D_T^{\rm reg}(t,\Delta\rho)+D_T^{\rm reg}(0,0). \tag{6.2}$$

Now the corrected experimental data correspond to our theoretical expressions $\overline{\eta}$ and D_T. In mode coupling theory the procedure is somewhat different, since there the complete background value of the transport coefficient is subtracted, which means, for the shear viscosity,

$$\begin{aligned}\Delta\overline{\eta}(t,\Delta\rho)&=\overline{\eta}^{\rm expt}(t,\Delta\rho)-\overline{\eta}^{\rm reg}(t,\Delta\rho)\\&=\overline{\eta}^{\rm corr}(t,\Delta\rho)-\overline{\eta}^{\rm reg}(0,0)\end{aligned} \tag{6.3}$$

(see Fig. 5 in Ref. [3]). A similar expression can be found for the thermal diffusivity ΔD_T. Inserting the theoretical expression for $\overline{\eta}^{\rm corr}(t,\Delta\rho)$ leads to a singular contribution $\Delta\overline{\eta}$ which is symmetric in $\Delta\rho$. This arises from the constant value of $\overline{\eta}_0$ in expression (3.1). Note that the mode coupling theory uses the full background value $\overline{\eta}^{\rm reg}(t,\Delta\rho)$ instead of $\overline{\eta}_0$, so that their expressions are not fully symmetric in $\Delta\rho$.

Let us now come back to the fit procedure: We start with the shear viscosity along the critical isochore, and choose t_0 far away from the critical point where $\overline{\eta}$ is given by its background value once that the experimental data were corrected corresponding to Eq. (6.1). Theoretically t_0 should go to infinity as only then the singular part completely vanishes. Practically, however, the choice depends on the region where experimental data are available as well as on experimental uncertainties [21]. Once t_0 is chosen, we can calculate Γ_0 as a function of f_0 inverting Eq. (2.6). With the values of t_0 and $\Gamma_0(f_0)$ we can fit f_0 in the nonasymptotic region with x_η kept at its one-loop value $\frac{1}{19}$. If possible it is better to move on to the experimental data for the thermal diffusivity along the critical isochore for this fit of f_0, as the thermal diffusivity depends only weakly on the exact value of x_η. With $\Gamma_0(f_0)$ and the set of parameters t_0 and f_0, we return to the data for the shear viscosity along the critical isochore and finally fit the exponent x_η in the asymptotic region. Therefore, it is advisable to use the expression for the average shear viscosity (4.1), as gravitational effects will have a significant influence on the shape of the curve. The theoretical results for the shear viscosity or thermal diffusivity along other isochores or isotherms then follow without any other free parameter. We should note here that if only data for the shear viscosity along the critical isochore are available a fit of both f_0 and x_η is not unerring, as $\overline{\eta}$ depends sensitively on both parameters. Only if the saturation value of the shear viscosity very close to the critical point is known from experiments may we express f_0 numerically in terms of x_η so that we can perform a one parameter fit along the critical isochore.

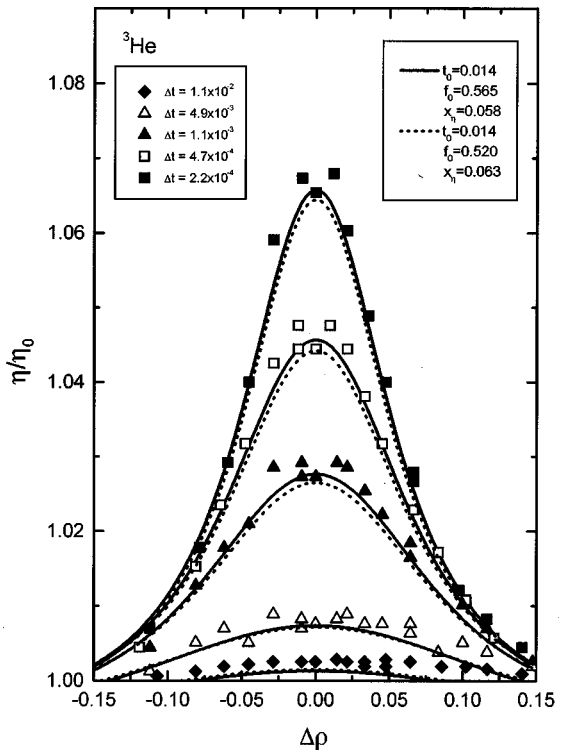

FIG. 8. Shear viscosity in ^{3}He along various isotherms. Full curves are for $x_\eta = 0.058$, and dotted curves for $x_\eta = 0.063$. Experimental data are from Ref. [20].

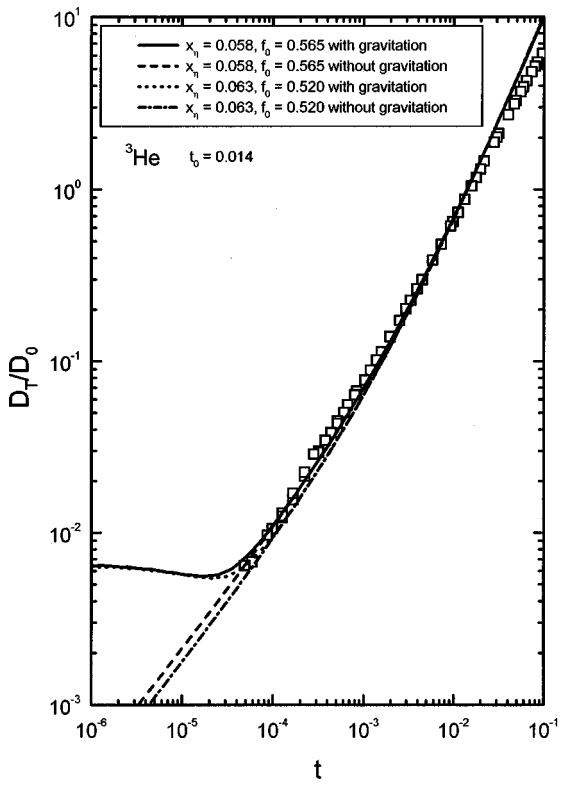

FIG. 9. Thermal diffusivity in ^{3}He along the critical isochore for $x_\eta = 0.058$ and 0.063 with gravitation (full and dotted curve) and without (dashed and dash-dotted curve). Experimental data are obtained from Ref. [23] as explained in the text.

A. Comparison with ^{3}He and ^{4}He

In Figs. 7–10 we compare the shear viscosity and thermal diffusivity with experimental data in ^{3}He and ^{4}He. We start with the normalized shear viscosity $\overline{\eta}/\overline{\eta}_0$ along the critical isochore, and compare our theoretical results with (full curve) and without (dash-dotted curve) gravitation with the ^{3}He and ^{4}He data of Agosta *et al.* [20] in Fig. 7, which can be compared with Fig. 13 of Ref. [20] where the experimental data are compared with the results of the mode coupling theory. Therefore, the parameters f_0 and x_η were fitted from the shear viscosity data, and for ^{3}He also from the thermal diffusivity data along the critical isochore as explained above. This leads to a value of the critical exponent $x_\eta = 0.058$.

In Fig. 8 we continue with a comparison of our theory for the renormalized shear viscosity along various isotherms with experimental ^{3}He data of Ref. [20]. A similar comparison of the ^{3}He data with the mode coupling theory is shown in Fig. 14 of Ref. [20]. Mind that the results for the density dependence, shown in Fig. 8, follow without any further free parameter. In Figs. 9 and 10 we compare the normalized thermal diffusivity D_T/D_0 along the critical isochore and along two isotherms with experimental data of ^{3}He which we obtained by dividing the thermal conductivity data of Figs. 5 and 8 of Ref. [23] by $\rho C_p(t,\Delta\rho)$ taken from the cubic model [24] with background constants from [25]. These experimental data are corrected for the regular density dependence, but contain the full temperature-dependent background given in Ref. [23]. Therefore, to the theoretical result [Eq. (3.2)] we have to add the temperature-dependent background term $D_T^{\rm reg}(T) - D_T^{\rm reg}(T_c)$. From Figs. 7–10 we can conclude that, using the same set of constants for all figures, we find very good agreement in the critical region. In particular, we find the critical exponent $x_\eta = 0.058$ somewhat larger than the value used in Ref. [20], $x_\eta = 0.054$, within the mode coupling theoretical expressions for the shear viscosity taken from Ref. [26].

Another procedure is to consider only the shear viscosity for a fixed value of the universal exponent. We choose $x_\eta = 0.063$, the value taken in mode coupling theory [3] for the fluids analyzed in Sec. VI B. Then another background value for the mode coupling constant f_0 is obtained together with perfect agreement of the shear viscosity with the experimental data (the difference from the fit found above is hardly visible in Fig. 7). However, differences are seen in the prediction of the density dependence of the shear viscosity along the isotherms shown in Fig. 8 (dotted curves) and in the thermal diffusivity along the critical isochore (see Fig. 9, dotted and dash-dotted curve), as well as in the density dependence of the thermal diffusivity (see Fig. 10, dotted curves). If instead we use the temperature-dependent thermal conductivity at a critical density to fix f_0, and then apply the value $x_\eta = 0.063$ for the critical exponent in the shear viscosity, the theoretical shear viscosity deviates clearly from the the experimental data (see Fig. 7, dashed curve).

The situation in ^{4}He is somewhat different from ^{3}He, since, lacking sufficient thermal conductivity data, we had to find the nonuniversal parameters from the shear viscosity alone. Therefore, we fixed the dynamical exponent x_η to the values found or fixed for ^{3}He, and adjusted only the initial value for the mode coupling f_0 after choosing the appropriate t_0 (the parameters found are listed in Table III). As ex-

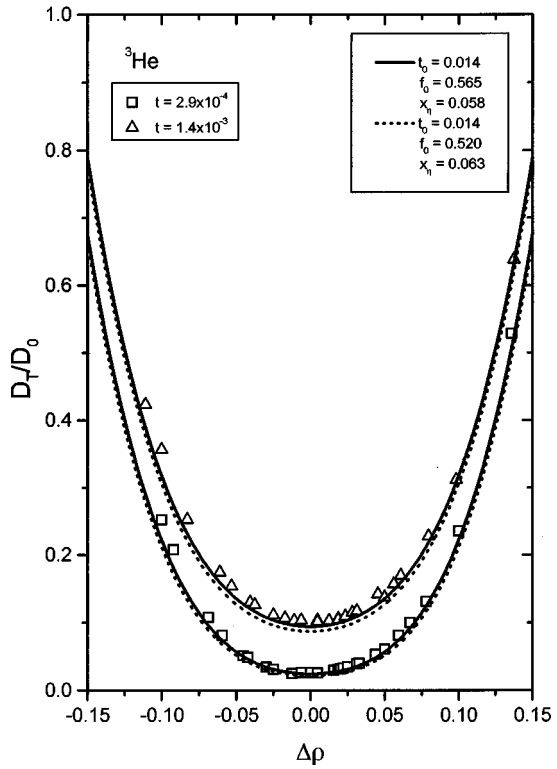

FIG. 10. Thermal diffusivity in ^{3}He along two isotherms. Full curves are for $x_\eta = 0.058$, and dotted curves for $x_\eta = 0.063$. Experimental data are from Ref. [23].

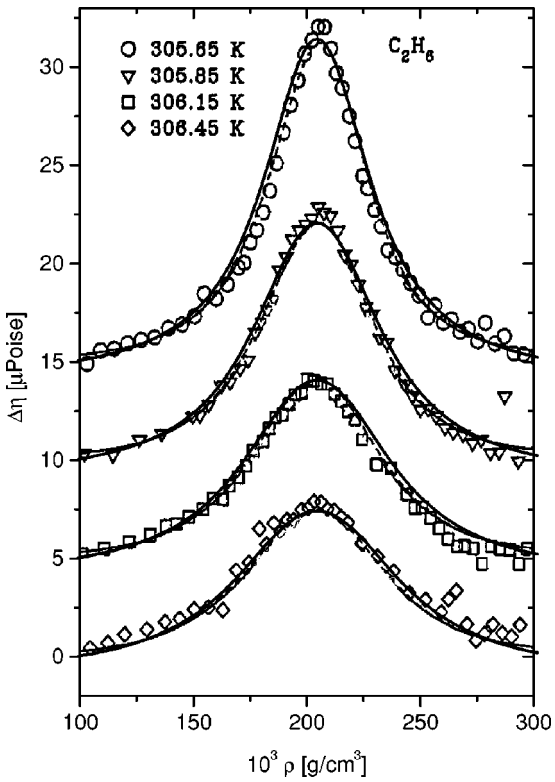

FIG. 11. Shear viscosity in C_2H_6 along various isotherms. The plot contains our results (thick curves) as well as experimental data [27] and theoretical results of the mode coupling theory (thin dashed curves) [3]. The curves were shifted by 5, 10, or 15 μP, respectively, for better clearness.

pected no conclusion on the *precise* value of x_η can be drawn. We finally remark here that the experimental shear viscosity data were divided by the full background $\overline{\eta}^{\rm reg}(t,\Delta\rho)$, whereas our theoretical expressions are divided by $\overline{\eta_0}$. Since in ^{3}He and ^{4}He the background is a rather smooth function this systematic error is negligible in the regions of temperatures and densities shown.

B. Comparison with C_2H_6 and CO_2

In Figs. 11–14 we finally compare our theoretical results with the mode coupling theory [3] and experimental data of CO_2 [27–29] and C_2H_6 [27,30] along various isotherms. We take the same value $x_\eta = 0.063$ for the critical exponent that has been used in mode coupling theory (smaller values showed less overall agreement with the data in our fits), for the other parameters see Table III. In Figs. 11 and 13 the singular part $\Delta\eta$ of the experimental data is plotted, which is identified with its theoretical counterpart

TABLE III. Initial values of the Onsager coefficient Γ_0 and the mode coupling f_0 at t_0 and value of the critical exponent x_η. For ^{3}He and ^{4}He, Γ_0 and f_0 are given for $x_\eta = 0.058$ and 0.063.

Liquid	t_0	$\Gamma_0 \times 10^{18}$(cm^4/s)	f_0	x_η
^{3}He	0.014	2.69	0.565	0.058
^{4}He	0.050	0.80	0.508	0.058
^{3}He	0.014	3.18	0.520	0.063
^{4}He	0.050	1.00	0.456	0.063
C_2H_6	0.100	6.20	0.576	0.063
CO_2	1.000	2.69	0.251	0.063

$$\Delta\eta^{\rm theor}(t,\Delta\rho) = \eta_0[g_\eta(t,\Delta\rho) - 1], \tag{6.4}$$

which is symmetrical around ρ_c, and indeed the experimental data show almost the same symmetry. We see that for the shear viscosity, mode coupling theory and RG theory yield the same quality of agreement in a surprisingly large region of densities.

For the thermal diffusivity, however, we are only able to describe the experimental data correctly within a density and temperature interval of $|\Delta\rho| < 0.2$ and $|t| < 0.01$, respectively, whereas the mode coupling theory covers a larger density and temperature range. The reason might be the following: Since we compare with the full experimental value of the thermal diffusion D_T but only the background values of the thermal conductivity are known, we need the specific heat at a constant pressure, which we take from the cubic model [24] with background constants from Ref. [31]. Then the experimental thermal diffusion is calculated from

$$D_T^{\rm theor}(t,\Delta\rho) = D_T^{\rm corr}(t,\Delta\rho) + \frac{\kappa^{\rm reg}(t,\Delta\rho)}{\rho C_p(t,\Delta\rho)} - \frac{\kappa^{\rm reg}(0,0)}{\rho C_p(t,\Delta\rho)}. \tag{6.5}$$

The specific heat expression we use is restricted to not too large values of t and $\Delta\rho$. Moreover, we use the asymptotic expression for the correlation length, which also breaks down in the background and leads to values of the thermal conductivity which are higher than the expected values (see, e.g., Fig. 8 in Ref. [2] for the deviation in ^{3}He). In fact the

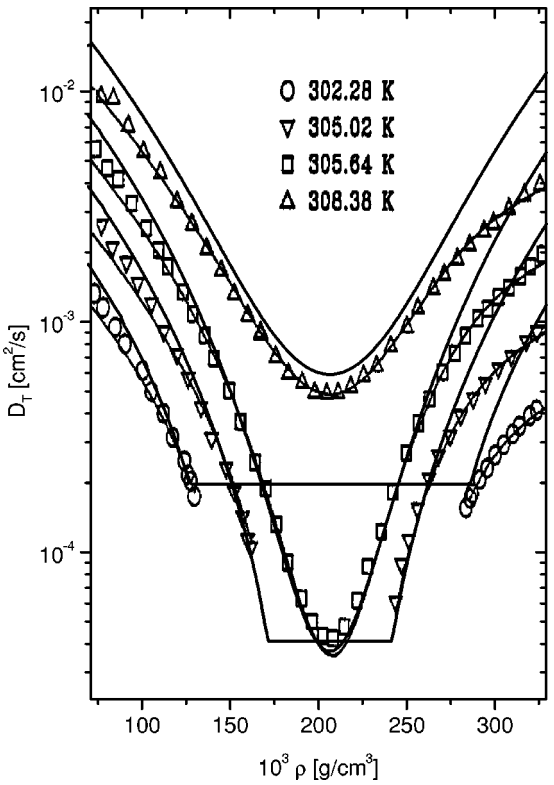

FIG. 12. Thermal diffusivity in C_2H_6 along various isotherms. The plot contains our results (thick curves) as well as experimental data [30] and theoretical results of the mode coupling theory (thin curves) [3]. We have used the analytic background expressions of Ref. [36].

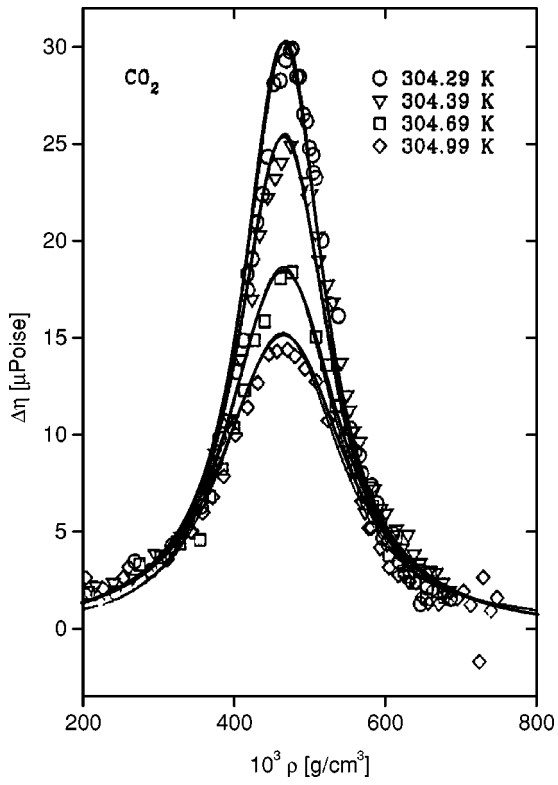

FIG. 13. Shear viscosity in CO_2 along various isotherms. The plot contains our results (thick curves) as well as experimental data [27] and theoretical results of the mode coupling theory (thin curves) [3].

correlation length is expected to saturate at some microscopic background value leading to temperature independent background values for the dynamic parameters [see Eqs. (2.3) and (2.4)]. In the mode coupling calculations this is taken into account relating the correlation length to the susceptibility [see Eqs. (4.31) and (4.32) in Ref. [3]].

VII. CONCLUSION

We have derived expressions for transport coefficients such as the shear viscosity and the thermal diffusivity within the field-theoretical method of the RG theory in one-loop order including the complex expression for the shear viscosity at finite frequency. As the flow parameter is a function of the correlation length only, we can include gravitational effects in full analogy to statics, so that we are able to describe the shear viscosity completely with only two free parameters, namely, the initial values of the Onsager coefficient and the mode coupling. In addition we may treat the exponent x_η, which is given by $\eta + x_\eta = 18/19 \sim 0.053$ in one-loop order, as an additional parameter correcting our one-loop crossover function for $\Gamma(t)$ for the true asymptotic behavior in the solution of the flow equation (2.4). Note that we effectively use the scaling law $\eta + x_\eta + x_\lambda = 1$, with $\eta = 0$, when we insert $\Gamma(t)$ into the thermal conductivity. However, this procedure keeps the theoretical expression for the Kawasaki amplitude and its asymptotic one-loop value $R^* = 1.056$.

Fitting the exponent x_η from experiments for ^{3}He we obtain the value 0.058 which is lower than other experimental values which are more near the two loop value $x_\eta = 0.065$ [11] or even higher [14,15] but in good agreement with other experimental fits in ^{3}He and ^{4}He [20]. In this paper we have pointed out that the value of the exponent x_η can be determined from the saturation value of the shear viscosity exactly at the critical point under the influence of gravitation when the parameter f_0 is taken from a fit of either the thermal diffusivity or that part of the data not influenced by gravity. Note added in proof: Recently the shear viscosity of xenon has been measured in a low gravity experiment [38]. The divergence is characterized by a critical exponent $x_\eta = 0.069 \pm 0.0006$, which was found from fits within the region $10^{-6} < t < 10^{-4}$. This result favors the two loop value for the exponent of the shear viscosity mentioned in [12].

ACKNOWLEDGMENTS

We thank H. Meyer for helpful discussions and for sending us experimental data, and R. F. Berg for sending us Ref. [38] prior to publication. This work was supported by the Fonds zur Förderung der wissenschaftlichen Forschung under Project No. P12422-TPH.

APPENDIX: CUBIC MODEL

The cubic model [32], an extension of the linear model introduced by Schofield [33], is an equation of state close to the critical point involving nonclassical critical exponents. The reduced temperature t, the reduced density $\Delta\rho$, and the

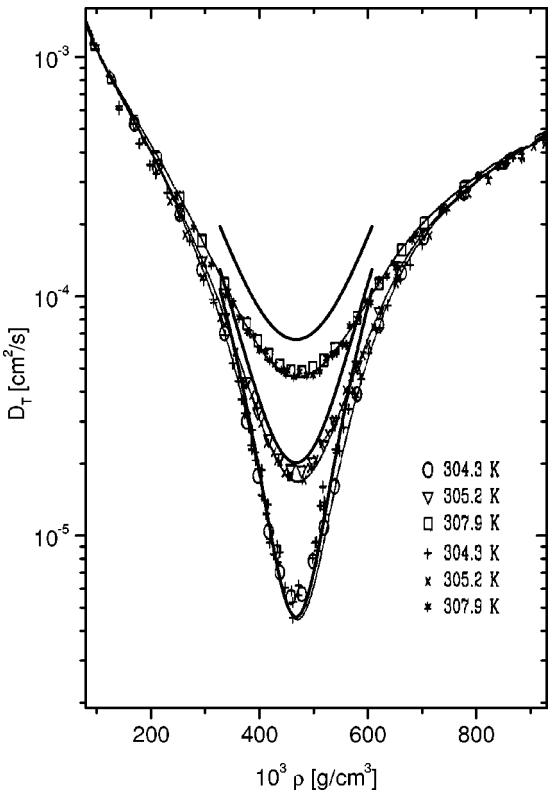

FIG. 14. Thermal diffusivity in CO_2 along various isotherms. The plot contains our results (thick curves) as well as experimental data [28,29] and theoretical results of the mode coupling theory (thin curves) [3]. We have used the analytic background expressions of Ref. [3] for the density dependence, and of Ref. [37] for the temperature dependence.

reduced chemical potential $\Delta\mu$ are expressed in terms of new variables r and θ,

$$t=\frac{T-T_c}{T_c}=(1-b^2\theta^2)r, \tag{A1}$$

$$\Delta\rho=\frac{\rho-\rho_c}{\rho_c}=k(\theta+c\theta^3)r^\beta, \tag{A2}$$

$$\Delta\mu=\frac{\mu-\mu_0(T)}{P_c/\rho_c}=a(\theta-\theta^3)r^{\beta\delta}, \tag{A3}$$

where $\mu_0(T)$ is the chemical potential along the critical isochore, which is assumed to be an analytic function of the temperature. The correlation length ξ is now given by the heuristic expression [24,34]

$$\xi=\xi_0(1+0.16\theta^2)r^{-\nu}=\xi_0 t^{-\nu}(1+0.16\theta^2)(1-b^2\theta^2)^\nu. \tag{A4}$$

Hence Eqs. (A1) and (A2) can be inverted numerically to obtain the correlation length as a function of the reduced temperature and the reduced density. We use the restricted cubic model [32] where the parameters $b^2=3/(3-2\beta)$ and $c=(2\beta\delta-3)/(3-2\beta)$ are connected to the universal critical exponents of Table II, so that the nonuniversality enters Eqs. (A1)–(A4) only via the constant parameters a, k and ξ_0 given in Table I.

The treatment of gravitational effects is in full analogy to statics, where it has been performed in detail by Hohenberg and Barmatz [35] within the linear model, and the extension in terms of the cubic model is straightforward so that we only mention the most important steps: Gravity enters the equation of state in terms of the chemical potential,

$$d\mu=-g\,d\hat{z}, \tag{A5}$$

where g is the gravitational constant and $\hat{z}$ the vertical coordinate in the vessel. Introducing the dimensionless vertical coordinate $z=\hat{z}/h$, where h is the height of the vessel, and choosing the origin of z along the coexistence line, we may integrate Eq. (A5) to obtain

$$\Delta\mu=-ghz. \tag{A6}$$

Inserting Eq. (A3) for the reduced chemical potential, Eq. (A6) may be inverted to obtain

$$z=-g_1(\theta-\theta^3)r^{\beta\delta}=-g_1 t^{\beta\delta}(\theta-\theta^3)(1-b^2\theta^2)^{-\beta\delta}, \tag{A7}$$

where $g_1=(aP_c)/(\rho_c gh)=h_c/h$ involves the constant ''critical height'' h_c also given in Table I. Since we have chosen the origin of z along the coexistence line, the phase transition always occurs at $z=0$ in our model, whereas the coordinates of the bottom and the top are functions of the temperature and the average density given by

$$\overline{\Delta\rho}=\int_{z_1}^{z_2}\Delta\rho(t,z)dz=\int_{\theta_1}^{\theta_2}\Delta\rho(t,\theta)\left(\frac{dz}{d\theta}\right)_t d\theta. \tag{A8}$$

Here z_1 and $z_2=z_1+1$ are the coordinates of the bottom and top of the vessel (in our units the height of the vessel is unity), and θ_1 and θ_2 the corresponding values of the cubic model variable θ, which can be found from Eq. (A7). Equation (A8) may then be inverted numerically to obtain θ_1 and θ_2 as a function of the reduced temperature and the average reduced density. Along the critical isochore, however, the situation becomes much easier as the coordinates of the bottom and top are then always given by $z_{1,2}=\mp 1/2$ which we simply insert into Eq. (A7) to obtain θ_1 and θ_2. Once θ_1 and θ_2 have been found we can insert these values into Eq. (A2) and Eq. (A4) to obtain the reduced density and the correlation length at the bottom $[\Delta\rho_b(t,\overline{\Delta\rho})=\Delta\rho(t,\theta_1)$, $\xi_b(t,\overline{\Delta\rho})=\xi(t,\theta_1)]$ and at the top $[\Delta\rho_t(t,\overline{\Delta\rho})=\Delta\rho(t,\theta_2)$, $\xi_t(t,\overline{\Delta\rho})=\xi(t,\theta_2)]$ of the vessel which we need for Eq. (4.1). The integral for the average thermal diffusivity (4.2) can now be written as

$$D_{T_{av}}(t,\overline{\Delta\rho})=\int_{z_1}^{z_2}D_T[\xi(t,\Delta\rho(z))]dz$$
$$=\int_{\theta_1}^{\theta_2}D_T(\xi(t,\theta))\left(\frac{\partial z}{\partial\theta}\right)_t d\theta, \tag{A9}$$

and may easily be integrated. To end this section let us note that we need an analytic expression for the specific heat at constant pressure $C_P(t,\Delta\rho)$ in terms of the cubic model in order to evaluate the thermal conductivity $\kappa_T(t,\Delta\rho)=\rho C_P D_T(t,\Delta\rho)$. Such an expression can be found, e.g., in Ref. [24], and the background constants entering theses equations are taken from Ref. [25] for ^{3}He and from Ref. [31] for CO_2 and C_2H_6.

[1] R. Folk and G. Moser, Phys. Rev. E **57**, 683 (1998).
[2] R. Folk and G. Moser, Phys. Rev. E **57**, 705 (1998).
[3] J. Luettmer-Strathmann, J. V. Sengers, and G. A. Olchowy, J. Chem. Phys. **103**, 7482 (1995).
[4] R. A. Ferrell, Phys. Rev. Lett. **24**, 1169 (1970).
[5] R. Perl and R. A. Ferrell, Phys. Rev. A **6**, 2358 (1972).
[6] S. B. Kiselev and V. D. Kulikov, Int. J. Thermophys. **15**, 283 (1994).
[7] T. Ohta, J. Phys. C **10**, 791 (1977).
[8] K. Kawasaki, Ann. Phys. (N.Y.) **61**, 1 (1970).
[9] R. Perl and R. A. Ferrell, Phys. Rev. Lett. **29**, 51 (1972); Phys. Rev. A **6**, 358 (1972).
[10] J. K. Bhattacharjee and R. A. Ferrell, Phys. Rev. A **28**, 2363 (1983).
[11] E. D. Siggia, B. I. Halperin, and P. C. Hohenberg, Phys. Rev. B **13**, 2110 (1976).
[12] Hong Hao, Ph.D. thesis, University of Maryland, College Park, Maryland, 1991 (cited in Ref. [3]).
[13] G. Paladin and L. Peliti, J. Phys. (France) Lett. **43**, 15 (1982), **45**, 289(E) (1984).
[14] R. F. Berg and M. R. Moldover, J. Chem. Phys. **93**, 1926 (1990).
[15] R. F. Berg and M. R. Moldover, Phys. Rev. A **42**, 7183 (1990).
[16] J. K. Bhattacharjee and R. A. Ferrell, Phys. Lett. **76A**, 290 (1980).
[17] J. K. Bhattacharjee and R. A. Ferrell, Phys. Rev. A **27**, 1544 (1983).
[18] R. Folk and G. Moser, Phys. Rev. Lett. **75**, 2706 (1995).
[19] R. Folk and G. Moser, Condens. Matter Phys. (Ukraine) **7**, 27 (1996).
[20] C. C. Agosta, S. Wang, L. H. Cohen, and H. Meyer, J. Low Temp. Phys. **67**, 237 (1987).
[21] Inspection of the experimental data shows that the ratio $\overline{\eta}/\overline{\eta}_0$ may be smaller than 1. Therefore, we adjust the temperature t_0 to this point. Then the only parameter remaining in the ratio is f_0. The value of Γ_0 is found from Eq. (2.6).
[22] J. V. Sengers and J. M. H. Levelt-Sengers, Annu. Rev. Phys. Chem. **37**, 189 (1986).
[23] E. Pittman, L. H. Cohen, and H. Meyer, J. Low Temp. Phys. **46**, 115 (1982).
[24] J. V. Sengers and J. M. H. Levelt Sengers, in *Progress in Liquid Physics*, edited by C. A. Croxton (Wiley, New York, 1978), Chap. 4.
[25] R. P. Behringer, T. Doiron, and H. Meyer, J. Low Temp. Phys. **24**, 315 (1976).
[26] G. A. Olchowy and J. V. Sengers, Phys. Rev. Lett. **61**, 15 (1988).
[27] H. Iwasaki and M. Takahashi, J. Chem. Phys. **74**, 1930 (1981); data are taken from Ref. [3].
[28] A. Michels, J. V. Sengers, and P. S. van der Gulik, Physica (Amsterdam) **28**, 1216 (1962); data are taken from Ref. [3].
[29] H. Becker and U. Grigull, Wärme Stoffübertrag. **11**, 9 (1978); data are taken from Ref. [3].
[30] P. Jany and J. Straub, Int. J. Thermophys. **12**, 165 (1987); data are taken from Ref. [3].
[31] Z. Y. Chen, A. Abbaci, S. Tang, and J. V. Sengers, Phys. Rev. A **42**, 4470 (1990).
[32] C.-C. Huang and J. T. Ho, Phys. Rev. A **7**, 1304 (1973).
[33] P. Schofield, Phys. Rev. Lett. **22**, 606 (1969).
[34] J. V. Sengers and J. M. J. van Leeuwen, Physica A **116**, 339 (1982).
[35] P. C. Hohenberg and M. Barmatz, Phys. Rev. A **6**, 289 (1972).
[36] V. Vesovic, W. A. Wakeham, J. Luettmer-Strathmann, J. V. Sengers, J. Millat, E. Vogel, and M. J. Assael, Int. J. Thermophys. **15**, 33 (1994).
[37] V. Vesovic, W. A. Wakeham, G. A. Olchowy, J. V. Sengers, J. T. R. Watson, and J. Millat, J. Phys. Chem. Ref. Data **19**, 763 (1990).
[38] R. F. Berg, M. R. Moldover, and G. A. Zimmerli, Phys. Rev. Lett. **82**, 920 (1999).